Optimum Passive Beamforming in Relation to Active-Passive Data Fusion

Bryan A. Yocom
Applied Research Laboratories
The University of Texas at Austin

Final Project
EE381K-14 – Multidimensional Digital Signal Processing
May 09, 2008

Abstract

One goal of active-passive data fusion is to combine the information collected by two types of sonar sensors to better perform signal processing. Active sensors, for example, give a good estimate of range, while passive sensors are most efficient at estimating the bearing and radiated spectrum of a contact. If it is assumed that prior information about the state of a contact has been collected in a data fusion framework, either by active sonar state estimates or by previous passive sonar state estimates, then the opportunity arises to direct the resources of a passive beamformer toward areas of high probability density. The modified beamformer can then provide a better estimate of the position of the contact. This paper seeks to find an optimum way of directing the resources of a passive horizontal line array when trying to estimate the direction of arrival (DOA), or bearing, of a contact. Various approaches are investigated including cued beamforming, minimum variance distortionless response (MVDR) beamforming, and robust capon beamforming (RCB). The resulting refinement in DOA estimation is compared to standard MVDR beamforming techniques. The scenarios in which cued beamforming outperforms surveillance beamforming are presented. Finally it is shown that although RCB does not currently outperform MVDR beamforming, much research is still needed.

I. INTRODUCTION

DATA fusion has become an increasingly popular topic in a number of fields [1]. One of its main goals is to use measurements from multiple sensors to better perform signal processing. Additionally, the integration of active and passive sonar systems is known to improve performance [2] because of the complementary information the two systems provide. Specifically, active sensors give a good estimate of range, while passive sensors are most efficient at estimating the bearing and radiated spectrum of a contact. It is therefore natural to apply data fusion to active and passive sonar systems.

Various types of beamformers have been used for passive sonar. The conventional (delay-and-sum) beamformer (CBF) is popular due to its simple implementation, but its precision is limited by the length of the array. Minimum variance distortionless response (MVDR) beamforming [3] can provide much greater precision, but it is sensitive to exact knowledge of the steering vector. The robust capon beamformer (RCB) [4] has addressed some of the sensitivities of MVDR and is therefore a prime candidate for data fusion. The focus of this paper will be on direction of arrival (DOA) estimation for underwater sonar using a passive, uniformly-spaced horizontal line array (HLA). The goal will be to design a beamformer that provides minimum error in DOA estimation while additionally providing a low entropy measurement. That is, the measurements should be both accurate and precise.

II. BACKGROUND

A. Minimum Variance Distortionless Response (MVDR) Beamforming

The MVDR beamformer was originally derived by Capon in 1969 [3]. Suppose we have a sampled array output given by $\mathbf{x}_n$, a replica vector $\mathbf{a}(\phi)$, and an estimated CSM, $\mathbf{R}_\mathbf{x}$, given by

$$\mathbf{R}_\mathbf{x} = \frac{1}{K}\sum_{i=1}^{K}\mathbf{x}_i\mathbf{x}_i^H \tag{1}$$

where i is the snapshot number and K is the number of snapshots used to approximate the CSM. It is assumed that K is large enough to ensure that $\mathbf{R}_\mathbf{x}$ is full rank. The optimization criteria are to minimize the output power while maintaining a distortionless response in the look direction.

In other words, the beamforming weights are found from the solution of

$$\min_{\mathbf{w}} \mathbf{w}^H \mathbf{R_x} \mathbf{w} \quad \text{subject to} \quad \mathbf{w}^H \mathbf{a}(\phi) = 1 \tag{2}$$

to be

$$\mathbf{w}_{MVDR}(\phi) = \frac{\mathbf{R_x}^{-1}\mathbf{a}(\phi)}{\mathbf{a}(\phi)^H \mathbf{R_x}^{-1}\mathbf{a}(\phi)}. \tag{3}$$

It should be noted that performing the inverse of the matrix $\mathbf{R_x}$ ($O(N^3)$ for an N element array) can be avoiding by solving for $\mathbf{y} = \mathbf{R_x^{-1}}\mathbf{a}(\phi)$ in $\mathbf{R_x}\mathbf{y} = \mathbf{a}(\phi)$ [5]. This can be done using a variety of linear equation solvers with complexity less than $O(N^3)$ since $\mathbf{R_x}$ is a Hermitian matrix.

The MVDR beamformer is very sensitive to mismatch between the actual and assumed DOA. Fig. 1 shows the squinting effect in which greater than unity response appears to one side of the contact when the steering vector is not perfectly matched to the true DOA. One common method

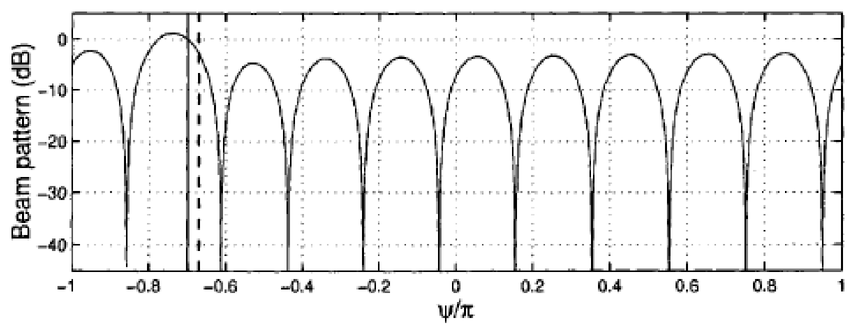

Figure 1. The "squinting" effect. The solid line is where the beamformer is steered to and the dotted line is the true DOA of the contact. As SNR becomes large this effect can become so strong that MVDR places a null of the beampattern at the true DOA of the contact in an attempt to minimize the output power. (Figure 6.26 from [6].)

of increasing the robustness of MVDR is to diagonally load $\mathbf{R_x}$ when calculating the weights in (3). That is, replace $\mathbf{R_x}$ with $\bar{\mathbf{R}}_\mathbf{x} = \mathbf{R_x} + \varepsilon\mathbf{I}$ where ε is a positive scalar. As ε is made large the sensitivity of the MVDR beamformer is decreased. This can be clearly seen by analyzing the form of the beamformer weights for exceedingly large diagonal loading: $\lim_{\varepsilon\to\infty} \mathbf{w}_{MVDR}(\phi) = \frac{\mathbf{a}(\phi)}{\mathbf{a}(\phi)^H\mathbf{a}(\phi)} = \mathbf{w}_{CBF}(\phi)$, which are simply the CBF weights. Unfortunately, it is not clear how to optimally choose ε. In practice, its value is often arrived at iteratively. This issue is addressed in Section IV-B.

B. Prior Information

Let us assume that prior information about the state of a contact has been collected in a data fusion framework, either by active sonar state estimates or by previous passive sonar state estimates. Additionally, assume that the only information available is the bearing from the array to the contact and that it is in the form of a one-dimensional continuous random variable, ϕ, with probability density function (PDF) $p(\phi)$. The generalization to multiple dimensions is trivial and therefore will not be considered at this time.

III. Bayesian Data Fusion Framework

Let us now discuss how beamformer measurements will be incorporated into the state estimate of a contact. The information that is provided by each measurement of the HLA is given by a likelihood function $L(\Phi|\phi)$, where $L(\Phi|\phi)$ represents the probability that the measurement Φ would occur given that the contact is actually at ϕ. If it is assumed that the signal and noise amplitudes are Gaussian random processes the likelihood function is given by [7]

$$L(\Phi|\phi) = c\exp\left\{K\gamma\sigma^2_{MVDR}(\phi)\right\} \tag{4}$$

where the constant, c, assures that the PDF sums to 1, the parameter γ is a function of the number of array elements and the SNR, and $\sigma^2_{MVDR}(\phi) = \mathbf{w}^H_{MVDR}(\phi)\mathbf{R_x}\mathbf{w}_{MVDR}(\phi)$ is the power estimate when MVDR beamforming is used. By a simple application of Bayes' rule, a new state estimate, $p(\phi|\Phi)$ (the posterior PDF), can be formed by combining the previous state estimate, $p(\phi)$ (the prior PDF), and the likelihood function, $L(\Phi|\phi)$:

$$p(\phi|\Phi) = \frac{L(\Phi|\phi)p(\phi)}{\int L(\Phi|\phi')p(\phi')d\phi'}. \tag{5}$$

This is a straightforward technique used by other authors, e.g. [7]. A measure for the amount of refinement given by $p(\phi|\Phi)$ can be given by the difference in *differential entropy* [8] between the prior and posterior PDF. The differential entropy is given by

$$H = \int_0^{\pi} p(\phi)\log_{10}(p(\phi))d\phi \tag{6}$$

and the entropy improvement (difference in differential entropy) by

$$\Delta H(\theta) = H_{prior} - H_{post}(\theta). \tag{7}$$

Here, the argument θ of H_{post} is referring to the actual DOA of the contact. The overall effectiveness of a passive beamformer can then be expressed as the expected value of the entropy improvement:

$$< \Delta H >= \int_0^\pi p(\theta)\Delta H(\theta)d\theta. \tag{8}$$

This technique was motivated in [9]. Although a positive value of $< \Delta H >$ indicates a refinement in the expected DOA estimate, it does not necessarily indicate refinement towards the actual DOA. The expected absolute error in DOA estimate,

$$< \Delta\phi >= \int_0^\pi p(\theta) \left| \arg\max_{\phi} \{p(\phi|\Phi,\theta)\} - \theta \right| d\theta, \tag{9}$$

gives a better indication of this [10]. In this case $p(\phi|\Phi,\theta)$ refers to the posterior PDF resulting from a measurement when the target is actually at θ.

IV. Passive Beamforming Approaches

A. Cued Beamforming

In [9], [10] an intuitive approach for concentrating (MVDR) beams in areas of high prior probability density was proposed. These *cued beams* were steered within a certain number of standard deviations from the mean of an assumed Gaussian prior PDF. The basic idea behind this approach was that there will be less of a chance for steering vector mismatch if the beams are closely spaced. Assuming that the number of cued beams equals the number of standard MVDR beams, a greater refinement in bearing could be obtained through an equal expenditure of computational resources. Although advantages have been seen in this technique, a continual spacing of maximum response axes (MRAs), based on the values of $p(\phi)$, would allow for the advantage of a full coverage of bearing. That is, MRAs should continually change from dense spacing in areas of high prior probability to sparse spacing in areas of low prior probability.

A generalized strategy for cuing beams is now presented. Given a prior PDF, $p(\phi)$, the cumulative distribution function (CDF) is given by $F(\phi) = \int_{-\infty}^{\phi} p(t)dt$ where $\phi \in [0, \pi]$. If it is assumed that $\phi(F)$ can be solved for (which is always the case when a PDF is discretized), we can define the MRA of the m^{th} beam according to

$$\Phi_m = \phi\left(\frac{m}{M-1}\right) \tag{10}$$

where $m \in \left\{ 0, \quad 1, \quad 2, \quad \ldots \quad M-1 \right\}$ is the beam number when there are M beams to be steered. The set of values in (10) will be referred to as our generalized cued beams.

B. Robust Capon Beamforming

The MVDR beamformer is also know as the Capon beamformer. As previously discussed, the Capon beamformer has long been known to suffer from sensitivity to mismatch. Only recently, though, have some authors derived beamformers that directly account for steering vector uncertainty [4], [11], [12], [13]. The robust Capon beamformer (RCB) presented in [4] is only slightly more computationally complex than the standard Capon beamformer. It's added complexity comes from an eigendecomposition of the N x N matrix $\mathbf{B}^H\mathbf{R}_\mathbf{x}^{-1}\mathbf{B}$ (complexity $O(N^3)$) and the solution of a Lagrange multiplier problem by the Newton-Raphson method (complexity varies depending on precision desired). The derivation of the RCB is beyond the scope of this paper, but the most important result is the beamforming weights,

$$\mathbf{w}_{RCB}(\phi) = \frac{\left(\mathbf{R}_\mathbf{x} + \frac{1}{\lambda}\mathbf{B}\mathbf{B}^H\right)^{-1}\bar{\mathbf{a}}(\phi)}{\bar{\mathbf{a}}^H(\phi)\left(\mathbf{R}_\mathbf{x} + \frac{1}{\lambda}\mathbf{B}\mathbf{B}^H\right)^{-1}\mathbf{R}_\mathbf{x}\left(\mathbf{R}_\mathbf{x} + \frac{1}{\lambda}\mathbf{B}\mathbf{B}^H\right)^{-1}\bar{\mathbf{a}}(\phi)}, \tag{11}$$

where $\bar{\mathbf{a}}(\phi)$ is the mean steering vector and λ is the Lagrange multiplier solution to the optimization problem (see [4] for intermediate steps). The N x L matrix $\mathbf{B}(\phi) = \left[\begin{array}{ccc} \bar{\mathbf{a}}(\phi) - \mathbf{a}(\phi_1) & \ldots & \bar{\mathbf{a}}(\phi) - \mathbf{a}(\phi_L) \end{array}\right]$ defines the uncertainty set for the steering vector where L is the number of samples of the array response near the mean response $\bar{\mathbf{a}}(\phi)$.

A couple important observations regarding (11) can be made. First of all, for exceedingly large λ, $\lim\limits_{\lambda\to\infty} \mathbf{w}_{RCB}(\phi) = \mathbf{w}_{MVDR}(\phi)$. Second, if $\mathbf{R}_\mathbf{x}$ is diagonally loaded as in Section II-A, then $\lim\limits_{\varepsilon\to\infty} \mathbf{w}_{RCB}(\phi) = \mathbf{w}_{CBF}(\phi)$. The significance of these limiting cases will be discussed in Section

VI.

C. Robust Capon Beamformer with Cued Beams

The RCB can naturally be extended to operate using the generalized cued beams given by (10). Since the cued beam MRAs will typically be unevenly spaced, the uncertainty set, given by matrix **B**, should also vary for each beam. More specifically, **B** should be constructed using samples of the array response that are between the two adjacent MRAs. The midpoint between two MRAs is a sufficient boundary for where to sample the array response for each beam. This approach will essentially vary the beamwidth of each beam based on its distance from adjacent beams, and, in doing so, help to ensure that the beams give a full coverage of bearing. Although finely spaced beams will not cover every bearing, all directions will be covered by at least one beam. If a contact is detected, the data fusion framework will trigger the cued beams to be steered in that direction. The same likelihood function, (4), will be used for the cued RCB (henceforth referred to as the CRCB) but with $\sigma^2_{MVDR}(\phi)$ replaced with $\sigma^2_{RCB}(\phi)$, the RCB power estimate.

V. Performance Analysis

Simulated data generated by the Sonar Simulation Toolset (SST) [14], [15] was used to assess the effectiveness of the RCB and CRCB in comparison to previous approaches using MVDR beamforming. The simulation involved a source 10 km away emitting a steady tone at 200 Hz, a constant sound speed profile of 1500 m/s, and a 34 element HLA of length 45 m. The element level SNR was -5 dB. The integrals in (8) and (9) were evaluated by simulating 500 sources evenly spaced in bearing over $0 < \theta < \pi$, where $\theta = 0, \pi$ are along the line of bearing of the HLA. In all cases the prior PDF was Gaussian with a mean of $\theta = \frac{\pi}{2}$. In addition, the generalized cued beams given by (10) were used whenever cued beams were specified. Finally, the MVDR plots are shown for the optimal level of diagonal loading.

There are a couple of important things to notice about Fig. 2. First, the cued beams always outperform the corresponding surveillance beams for sufficiently narrow prior PDFs. That is, there is greater expected entropy improvement and less expected DOA error. This is expected because the finer spacing of MRAs should ensure that there is less mismatch between a beam

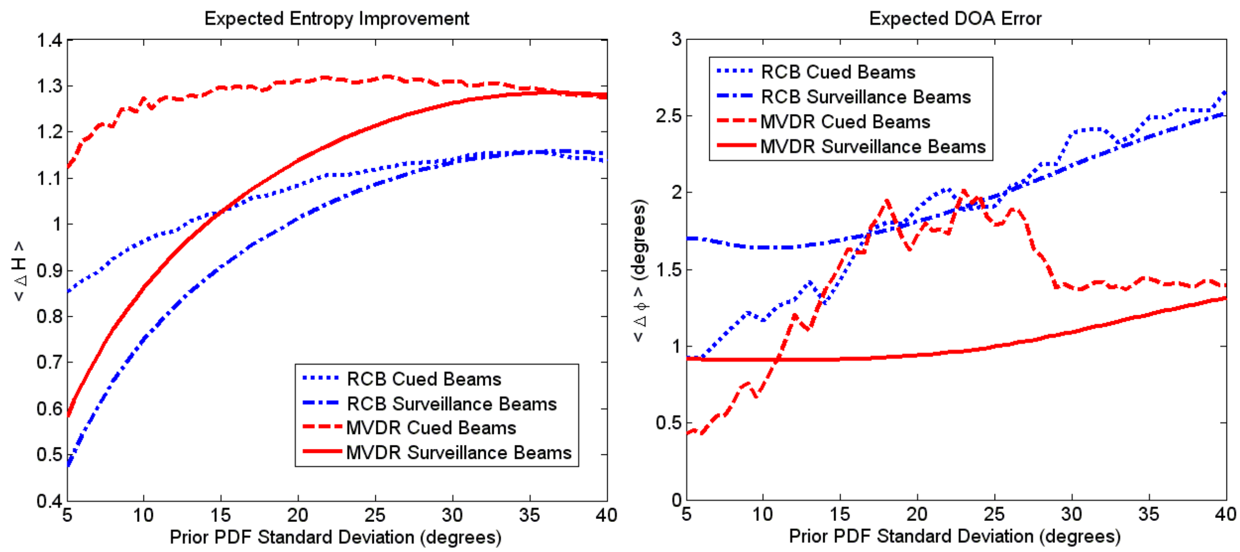

Figure 2. Expected Entropy Improvement and DOA Error shown as a function of prior PDF standard deviation. The surveillance beams were spaced uniformly in $\cos(\phi)$ as is common practice in surveillance beamforming.

MRA and the true location of a contact. In addition, expected entropy improvement decreases as the prior PDF becomes more narrow. This shows that there is a limit to the amount of refinement that can be achieved. If the prior PDF width is comparable to the width of the beams then further refinement cannot be obtained. Also notice that the performance of the cued beams approaches that of the surveillance beams for wide prior PDFs. This is to be expected because the cued beams should approach the spacing of the surveillance beams as the prior approaches a uniform PDF. Another important observation is that the expected DOA error for cued beams is actually worse than the surveillance beams for wider prior PDFs. This shows that cuing beams can actually be disadvantageous when the prior PDF is not sufficiently narrow.

The final important observation is that the MVDR beamformers actually outperform the RCBs in most cases. There are a few possible reasons for this. One is that there are different amounts of noise in each beam of the RCB (and CRCB) because the beamwidths differ. This problem was confirmed experimentally by observing peaks in the likelihood function at angles where the beams were widest, even though no contacts were present in the specified direction. The problem could be accounted for by weighting each beam's output in relation to its beamwidth. In the plots shown the RCB beams were weighted by a value inversely proportional to the beamwidth. This method is admittedly *ad hoc* and is only being used until a method based more in theory is developed. Another reason for the poor performance of the RCBs is that the parameter γ in (4) is SNR dependent. The value of γ essentially controls how much peaks in the beamformer output are emphasized. Experiments showed that the RCBs demonstrated considerable sensitivity to this parameter in comparison to MVDR beamforming.

VI. Conclusions and Future Work

In order to measure the performance of the CRCB the expected entropy improvement and expected absolute DOA error were analyzed. With respect to these measures, the new design did not perform as well as the author had hoped. There is still much research to be done, though. As previously mentioned, the CRCB beams should be weighted such that the noise gain is uniform across beams. The parameter γ in (4) also needs to be optimally selected. In addition, it would be informative to find the optimal number of samples of the array response, L, to use in the uncertainty set given by matrix $\mathbf{B}$ of the CRCB. Given the proper choices for these design parameters the CRCB could outperform the cued MVDR beamformer.

The performance measures presented here are for a very simple scenario. For example, there are no interferers and the target is not moving. A fairer evaluation of performance would require implementation in an actual data fusion framework. One aspect of the data fusion process that was not discussed in this paper is the use of the posterior PDF resulting from one measurement from the HLA as the prior PDF for a subsequent measurement. In other words, the passive beamformer can be used in a feedback configuration, fusing prior measurements with current measurements. Preliminary evaluation of this configuration has shown that the CRCB can provide lower entropy measurements than the cued MVDR beamformer after multiple feedback iterations (with similar DOA error). This is only true when the state estimate (given by the current posterior PDF) is stationary in its mean. The MVDR beamformer and CBF, on the other hand, have been observed to be robust to mean stationarity. That is, regardless of the shape and stationarity of the prior PDF, the state estimate will eventually converge such that its mean corresponds to the true DOA of the contact.

Although mean stationarity was not previously discussed, it is a parameter that can easily be provided by a well structured data fusion framework. For a HLA it would correspond to the bearing rate, that is, the velocity in bearing of the DOA estimate. Future work regarding the RCB therefore could involve decreasing its sensitivity in proportion to the bearing rate. This might be done by increasing the factors ε and λ discussed in Section IV-B so that the RCB becomes a detuned version that approaches the behavior of the MVDR beamformer or CBF. Future work regarding cued beams might involve modifying the generalized cued beams strategy to take into account the bearing rate. Specifically, there should be less emphasis on cuing the beams if the bearing rate is high.

Finally, this paper has made it apparent that other performance measures need to be developed to properly evaluate the effectiveness of a beamformer when used in data fusion. These would be required for both the feedback configuration discussed and for cases when active sonar sensors are added to the data fusion. Some of these measures might include state convergence rate, minimum detectable level (in terms of SNR), minimum achievable entropy, and minimum achievable DOA error.

REFERENCES

[1] D. Hall and J. Llinas, "An introduction to multisensor data fusion," *Proc. IEEE*, vol. 85, no. 1, pp. 6–23, Jan. 1997.

[2] S. Stergiopoulos, "Implementation of adaptive and synthetic-aperture processing schemes in integrated active-passive sonar systems," *Proc. IEEE*, vol. 86, no. 2, pp. 358–398, Feb. 1998.

[3] J. Capon, "High-resolution frequency-wavenumber spectrum analysis," *Proc. IEEE*, vol. 57, no. 8, pp. 1408–1418, Aug. 1969.

[4] J. Li, P. Stoica, and Z. Wang, "On robust capon beamforming and diagonal loading," *IEEE Trans. Signal Process.*, vol. 51, no. 7, pp. 1702–1715, Jul. 2003.

[5] B. L. Evans, Apr. 2008, personal dialogue.

[6] H. L. Van Trees, *Detection, Estimation, and Modulation Theory, Part IV, Optimum Array Processing*. New York: Wiley, 2002.

[7] K. L. Bell, Y. Ephraim, and H. L. Van Trees, "A Bayesian approach to robust adaptive beamforming," *IEEE Trans. Signal Process.*, vol. 48, no. 2, pp. 386–398, Feb. 2000.

[8] M. A. Mattar, M. R. Rudary, and E. W. Weisstein, "Differential entropy," *From MathWorld – A Wolfram Web Resource*, 2008. [Online]. Available: http://mathworld.wolfram.com/DifferentialEntropy.html

[9] T. W. Yudichak, B. A. Yocom, and M. Le, "Cued beamforming of passive arrays in the context of active-passive data fusion," in *J. Acoust. Soc. Am.*, vol. 122, no. 5, Nov. 2007, p. 3073.

[10] ——, "Cued passive bearing estimation in distributed sensor data fusion," in *Proc. Int. Conf. on Information Fusion*, Cologne, Germany, Jul. 2008.

[11] S. Vorobyov, A. Gershman, and Z.-Q. Luo, "Robust adaptive beamforming using worst-case performance optimization: a solution to the signal mismatch problem," *IEEE Trans. Signal Process.*, vol. 51, no. 2, pp. 313–324, Feb. 2003.

[12] R. Lorenz and S. Boyd, "Robust minimum variance beamforming," *IEEE Trans. Signal Process.*, vol. 53, no. 5, pp. 1684–1696, May 2005.

[13] C. Ma, B. P. Ng, H. Bao, and X. Yang, "Robust adaptive beamforming for large steering angle error," in *Proc. IEEE Int. Symp. on Circuits and Systems*, vol. 3, May 2004, pp. III–273–6.

[14] R. P. Goddard, "The Sonar Simulation Toolset, Release 4.1: Science, Mathematics, and Algorithms," Applied Physics Laboratory, University of Washington, Seattle, Tech. Rep. APL-UW 0404, Mar. 2005.

[15] ——, "The sonar simulation toolset," in *Proc. OCEANS*, vol. 4, Sep. 1989, pp. 1217–1222.